

Matrix-Isolation Studies of the Reactions of Ground- and Excited-State Atomic Iron with Cyclopropane

C. Judith Chu, Zakya H. Kafafi, John L. Margrave, Robert H. Hauge, and W. E. Billups*

Department of Chemistry, Rice University, Houston, Texas 77005-1892

Received June 22, 1999

The chemistry of atomic iron reacting with cyclopropane in an argon matrix at 15 K has been investigated. A spontaneous reaction leads to the formation of $\text{C}_2\text{H}_4\text{FeCH}_2$, $[\text{Fe}(\text{C}_2\text{H}_2)]\text{[CH}_4\text{]}$, and a species in which FeH_2 is complexed with allene, $(\text{FeH}_2)(\text{H}_2\text{C}=\text{C}=\text{CH}_2)$. UV photolysis of the matrix resulted in C–H bond activation to give methylvinyliron and ethynyliron hydride. Atomic iron was observed to form a weakly bound adduct with cyclopropane. This adduct is stable to irradiation using visible light, but UV photolysis led to enhanced absorptions assigned to methylvinyliron, ethynyliron hydride, and methane. A strongly interacting complex between two cyclopropane molecules and iron was observed. This species exhibits a large carbon–hydrogen frequency shift that is suggestive of an agostic hydrogen interaction. This complex undergoes a photoreaction at $\lambda \geq 500$ nm to yield the disproportionation product $\text{Fe}(\text{C}_2\text{H}_4)_3$, isolated for the first time in an argon matrix. Photolysis of $\text{Fe}(\text{C}_2\text{H}_4)_3$ results in the loss of ethylene to form $\text{Fe}(\text{C}_2\text{H}_4)_2$.

Introduction

Previous work on the activation of cyclopropane by transition metals has shown that the metal usually inserts into a carbon–carbon bond, forming a metallacyclobutane.¹ The unligated metallacycle, nickelacyclobutane, was formed when nickel atoms were cocondensed with cyclopropane in an argon matrix at 15 K.² Metathesis of the metallacycle occurs during photolysis using $\lambda \geq 500$ nm irradiation to form $(\text{C}_2\text{H}_4)\text{NiCH}_2$, a species in which ethylene is bound to NiCH_2 as a π complex. In contrast, we have found that the reactions of iron and cyclopropane are significantly more complex. In this paper, we describe the chemistry, including photolysis studies, of iron atoms reacting with cyclopropane in an argon matrix at 15 K.

Experimental Section

A detailed description of the matrix-isolation apparatus interfaced to a vacuum IBM IR-98 Fourier transform spectrometer has been published.³ Iron metal was placed inside an alumina crucible enclosed in a tantalum furnace. Iron vapor was then obtained by resistively heating the tantalum furnace over the range 1150–1450 °C, as determined by a microoptical pyrometer (Pyrometer Instrument Co.). The concentration of iron (Aesar, 99.98%) was varied from 0 to 20 parts per thousand of argon (Matheson, 99.9998%), while the concentration of cyclopropane (Matheson, 99.0% minimum) was varied from 0 to 11 parts per thousand of argon. A quartz crystal microbalance was used to determine the rates of deposition of iron, cyclopropane, and argon.

Cyclopropane and iron atoms were codeposited in excess argon onto a polished rhodium-plated copper surface. A closed-

Table 1. FTIR Frequencies (cm^{-1}) for C_3H_6 and C_3D_6 Recorded in Solid Argon

vibrational mode	C_3H_6	C_3D_6
ν_1 , CH_2 or CD_2 s-stretch	3038 (R) ^a	2236 (R)
ν_2 , CH_2 or CD_2 scissors	1479 (R)	1274 (R)
ν_3 , ring stretch	1188 (R)	956 (R)
ν_4 , CH_2 or CD_2 twist	1124.8	747.8
ν_5 , CH_2 or CD_2 wag	1063.1	883.5
ν_6 , CH_2 or CD_2 a-stretch	3091.8	2329.4
ν_7 , CH_2 or CD_2 rock	864.7	611.8
ν_8 , CH_2 or CD_2 s-stretch	3016.6	2208.3
ν_9 , CH_2 or CD_2 scissors	1434.3	1068.1
ν_{10} , CH_2 or CD_2 wag	1025.0	891.2
ν_{11} , ring deformation	875.3	714.4
ν_{12} , CH_2 or CD_2 a-stretch	3082 (R)	2329 (R)
ν_{13} , CH_2 or CD_2 twist	1188 (R)	940 (R)
ν_{14} , CH_2 or CD_2 rock	739 (R)	528 (R)

^a Frequencies for Raman-active modes (R) of C_3H_6 (g) and C_3D_6 (g) were obtained from ref 11.

cycle helium refrigerator was used to maintain the surface at 15 K. After a 30 min deposition, the matrix block was rotated 180° and an infrared spectrum was measured over the range 4000–500 cm^{-1} with an IBM IR-98 Fourier-transform infrared spectrometer. Similar experiments were carried out using deuterated cyclopropane (MSD Isotopes, 98.0% minimum). Photolyses were carried out after deposition of the reactants by exposing the matrices to a medium-pressure 100 W Hg lamp. A water Pyrex filter with Corning cutoff filters ($\lambda \geq 400$ and $\lambda \geq 500$ nm) and a band-pass filter in the range 280 nm $< \lambda < 360$ nm were used in these experiments.

Results

The FTIR spectra of cyclopropane and cyclopropane- d_6 recorded in solid argon at 15 K (4000–500 cm^{-1}) were obtained for reference purposes and these frequencies are listed in Table 1. New absorptions appeared throughout the 2000–600 cm^{-1} region when iron atoms were cocondensed with cyclopropane in excess argon at 15 K.

(1) Jennings, P. W.; Johnson, L. L. *Chem. Rev.* **1994**, *94*, 2241.

(2) Kline, E. S.; Hauge, R. H.; Kafafi, Z. H.; Margrave, J. L. *Organometallics* **1988**, *7*, 1512.

(3) Hauge, R. H.; Fredin, L.; Kafafi, Z. H.; Margrave, J. L. *Appl. Spectrosc.* **1986**, *40*, 588.

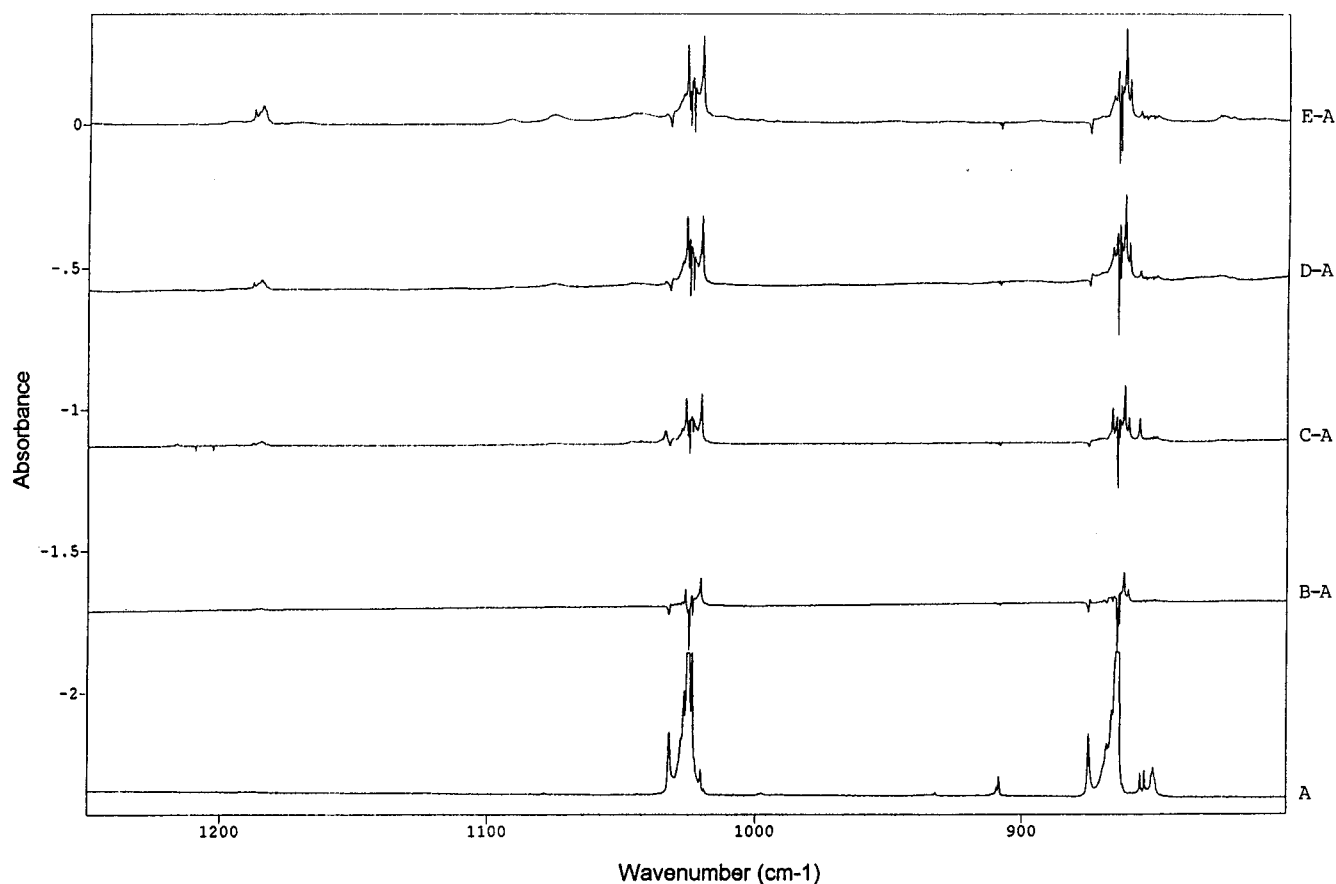


Figure 1. Iron concentration study. Infrared plots of Fe/C₃H₆/Ar matrices where the iron concentration (molar ratio) is increased gradually: (A) Fe/C₃H₆/Ar = 0/11/1000; (B) Fe/C₃H₆/Ar = 3.6/11/1000; (C) Fe/C₃H₆/Ar = 6.5/11/1000; (D) Fe/C₃H₆/Ar = 8.3/10/1000; (E) Fe/C₃H₆/Ar = 20/10/1000.

The growth of these absorptions with increasing iron concentration is shown in Figure 1. These spectra are presented as subtraction spectra, where the absorptions exhibited by the free cyclopropane have been subtracted. Positive peaks with respect to the baseline are those of newly formed species. The iron–cyclopropane concentration studies and photolysis experiments illustrate the complexity of these reactions, as shown by the different photolytic behavior of each product. Identification of the products required extensive studies on the reactions of iron with other small hydrocarbons, including methane, ethylene, and acetylene. Numerous experiments were undertaken to elucidate the chemistry of these reactions, including experiments with deuterated cyclopropane.

Cocondensation Products. The main product gave rise to bands adjacent to the cyclopropane absorptions (Figure 1). The most intense absorptions were observed as small perturbations in the ν_2 (CH₂ rock), ν_{10} (CH₂ wag), ν_9 (CH₂ scissor), ν_6 (CH₂ a-stretch), and ν_8 (CH₂ s-stretch) frequencies of cyclopropane, indicative of a hydrogen complexed iron–cyclopropane adduct. The subtraction spectra illustrated in Figure 1 show the growth of this species as the concentration of iron was increased. This study indicates that the iron/cyclopropane concentration increases linearly with iron concentration, in keeping with its assignment as a 1:1 iron/cyclopropane complex. The measured FTIR frequencies of this complex are listed in Table 2 along with those of free cyclopropane and a second complex in which iron is complexed to two cyclopropane molecules (discussed

Table 2. FTIR Frequencies (cm⁻¹) for Cyclopropane, Fe(C₃H₆), and Fe(C₃H₆)₂ in Solid Argon

vibrational mode	obsd C ₃ H ₆	obsd Fe(C ₃ H ₆)	obsd Fe(C ₃ H ₆) ₂ (d)
ν_6 , CH ₂ a-stretch	3091.8	3090.6 3089.1	
ν_7 , CH ₂ rock	864.7	862.2 860.6	
ν_8 , CH ₂ s-stretch	3016.6	3015.4 3013.9	2761.4 2755.5
ν_9 , CH ₂ scissors	1434.3	1434.0 1432.4	
ν_{10} , CH ₂ wag	1025.0	1026.2 1020.4	1091.9 1075.6
ν_{11} , ring deformation	875.3		

below). As expected, the frequency shifts for the 1:1 adduct are small, 1–5 cm⁻¹, reflecting the weak bonding in the complex. No perturbation was observed for the ring deformation mode of cyclopropane.

Other less intense bands have been assigned to the products labeled a–e in Figures 2 (2000–500 cm⁻¹) and 3 (3200–2700 cm⁻¹). The intensities of these bands are much weaker than the cyclopropane absorptions.

Absorption bands characteristic of transition-metal–olefin π complexes (peak a, Figure 2) were observed in the CH₂ scissoring region at 1184.8, 1186.1, and 1187.8 cm⁻¹. Other bands that correlate with peak a were observed in the CH₂ wagging mode region at 825.3 and 826.4 cm⁻¹. These absorptions increased linearly as the concentration of iron was increased. On the basis of

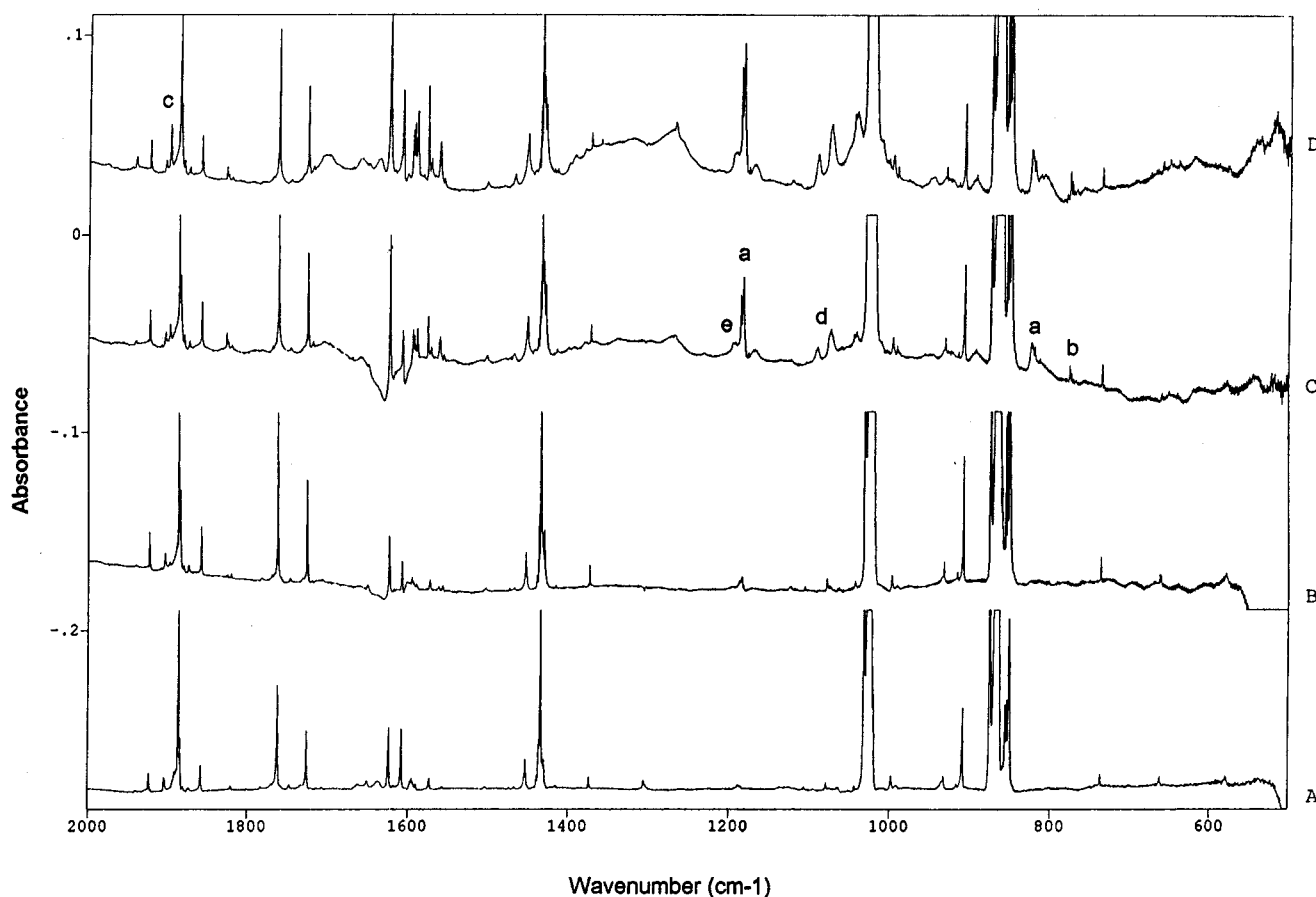


Figure 2. Absorptions arising from minor products a–e in the 600–2000 cm^{-1} region as the molar concentration of Fe is increased gradually: (A) Fe/C₃H₆/Ar = 0/11/1000; (B) Fe/C₃H₆/Ar = 3.6/11/1000; (C) Fe/C₃H₆/Ar = 12.8/10/1000; (D) Fe/C₃H₆/Ar = 20/10/1000.

Table 3. FTIR Frequencies (cm^{-1}) for (C₂H₄)FeCH₂, (C₂H₄)NiCH₂, FeCH₂, and C₂H₄ in Solid Argon^a

vibrational mode	FeCH ₂ ^b	(C ₂ H ₄)-NiCH ₂ ^c	obsd (C ₂ H ₄)-FeCH ₂ (a)	C ₂ H ₄ ^d
CH ₂ s-stretch	2941.6			2995.4
CH ₂ a-stretch	3011.5			3112.1
C=C stretch		1515.8	1469.9 (sh)	1629
		1514.3	1468.5	
CH ₂ scissors (ethylene)		1246.8	1187.8	1440.3
		1241.0	1186.1	
			1184.8	
CH ₂ wag (methylene)	700.3	795.5		
		784.2		
CH ₂ wag (ethylene)			826.4	947.4
			825.3	
M=C stretch	623.9	670.9	657.5 (broad)	
			653.1	

^a The most intense frequencies are noted in boldface type.

^b Reference 4. ^c Reference 2. ^d Reference 6.

concentration studies and by comparison of the absorption frequencies with other, previously characterized compounds, product a can be identified as (C₂H₄)FeCH₂, a species in which ethylene is coordinated with FeCH₂ as a π complex. The frequencies of (C₂H₄)FeCH₂⁴ and the nickel complex (C₂H₄)NiCH₂² are presented in Table 3 for comparison. The C=C stretching and CH₂ scissoring bands of ethylene at 1468.5 and 1184.8 cm^{-1} are in agreement with those observed for ethylene in (C₂H₄)-

NiCH₂. A shift to lower frequency by approximately 50 cm^{-1} has been observed for each mode, indicating that the π interaction between iron and ethylene is weaker than that between nickel and ethylene. The Fe=C stretching frequency at 653.1 cm^{-1} is in agreement with that observed for FeCH₂.⁴ The formation of (C₂H₄)FeCH₂ could be enhanced by photolysis using $\lambda \geq 500$ nm light but decreased with $\lambda \geq 400$ and $280 \text{ nm} \leq \lambda \leq 360 \text{ nm}$ irradiation. The photolytic behavior of (C₂H₄)FeCH₂ is discussed in greater detail below.

In contrast to the iron–cyclopropane chemistry, the reactions of atomic iron with deuterated cyclopropane are simpler in that only the π complex (C₂D₄)FeCD₂ is formed. The frequencies assigned to (C₂D₄)FeCD₂ and (C₂D₄)NiCD₂ from a previous study are summarized in Table 4. Another set of bands (peak b, Figure 2) at 778.4, 775.8, and 770.3 cm^{-1} increased linearly as the concentration of iron and cyclopropane was increased. In contrast to peak a, these absorptions increased initially during photolysis using $\lambda \geq 500$ nm light but remained constant with $\lambda \geq 400$ nm irradiation. These absorptions are in the C–H deformation region of transition-metal–acetylene π complexes. Comparisons with similar complexes suggest that assignment of peak b to an acetylene π complex coordinated to methane, (C₂H₂)Fe[CH₄], is plausible. The infrared frequencies of b along with those measured for the Ni(C₂H₂)⁵ complex are summarized in Table 5. Peaks labeled c (Figure 2) have been

(4) Chang, S.-C.; Hauge, R. H.; Kafafi, Z. H.; Margrave, J. L.; Billups, W. E. *J. Am. Chem. Soc.* **1988**, *110*, 7975.

(5) Kline, E. S.; Kafafi, Z. H.; Hauge, R. H.; Margrave, J. L. *J. Am. Chem. Soc.* **1987**, *109*, 2402.

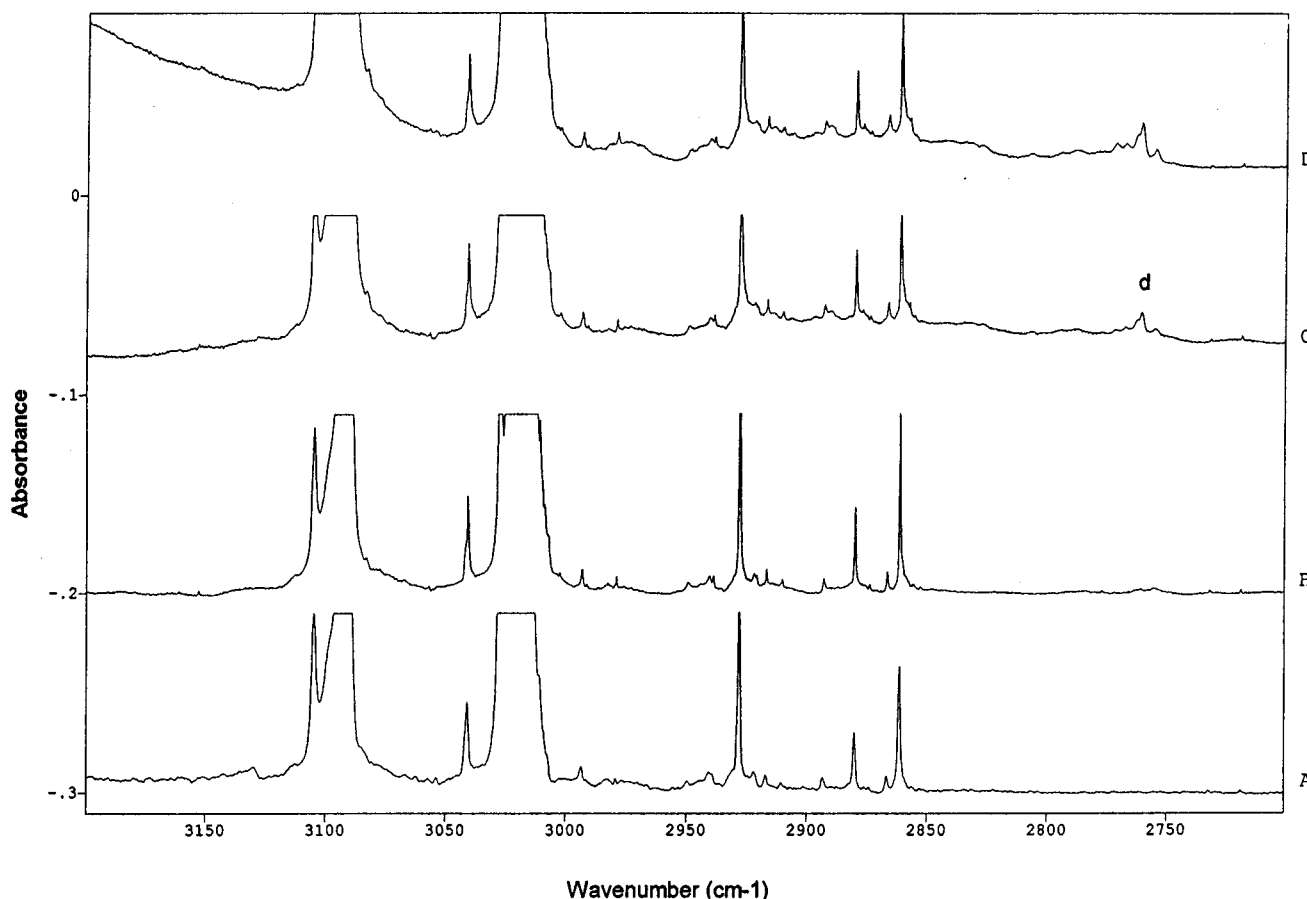


Figure 3. Absorptions arising from the minor product d in the 2700–3200 cm^{-1} region as the molar concentration of Fe is increased gradually: (A) $\text{Fe}/\text{C}_3\text{H}_6/\text{Ar} = 0/11/1000$; (B) $\text{Fe}/\text{C}_3\text{H}_6/\text{Ar} = 3.6/11/1000$; (C) $\text{Fe}/\text{C}_3\text{H}_6/\text{Ar} = 12.8/10/1000$; (D) $\text{Fe}/\text{C}_3\text{H}_6/\text{Ar} = 20/10/1000$.

Table 4. FTIR Frequencies (cm^{-1}) for $(\text{C}_2\text{D}_4)\text{FeCD}_2$ and $(\text{C}_2\text{D}_4)\text{NiCD}_2$ in Solid Argon^a

vibrational mode	$(\text{C}_2\text{H}_4)\text{-NiCH}_2^b$	$(\text{C}_2\text{D}_4)\text{-NiCD}_2^b$	obsd $(\text{C}_2\text{H}_4)\text{-FeCH}_2$ (a)	obsd $(\text{C}_2\text{D}_4)\text{-FeCD}_2$ (a)
CH_2 stretch		2215.6 2158.9		
$\text{C}=\text{C}$ stretch	1515.8 1514.3	1365.6	1469.9 (sh) 1468.5	1294.7
CH_2 scissors (methylene)	1023.3			
CH_2 scissors (ethylene)	1246.8 1241.0	954.6	1187.8 1186.1 1184.8	934.3
CH_2 wag (methylene)	795.5 784.2	615.9		528.2
CH_2 wag (ethylene)			826.4 825.3	628.2
$\text{M}=\text{C}$ stretch	670.9	648.5	657.5 (broad) 653.1	

^a The most intense frequencies are noted in boldface type.

^b Reference 2.

assigned tentatively to the FeH_2 complex (Scheme 1) of allene, $(\text{FeH}_2)(\text{H}_2\text{C}=\text{C}=\text{CH}_2)$. The absorption band at 1897.8 cm^{-1} is in the $\text{C}=\text{C}=\text{C}$ asymmetric stretching region of allene. A second band at 1658.2 cm^{-1} in the $\text{Fe}-\text{H}$ stretching region compares favorably with free FeH_2 at 1661.0 cm^{-1} . These absorptions increased linearly as the concentration of iron was increased. Comparisons of the frequencies measured for this complex with those of allene and propadienyliron hydride, $\text{HFeCH}=\text{C}=\text{CH}_2$,¹² are shown in Table 6. Broad absorption bands (peaks labeled d, Figure 2) at 1091.9

Table 5. FTIR Frequencies (cm^{-1}) for Acetylene, $[\text{Fe}(\text{C}_2\text{H}_2)][\text{CH}_4]$, and $\text{Ni}(\text{C}_2\text{H}_2)^a$

vibrational mode	C_2H_2	$\text{Ni}(\text{C}_2\text{H}_2)^a$	$[\text{Fe}(\text{C}_2\text{H}_2)][\text{CH}_4]$ (b)
in-plane CH s-bend		847.3	778.4
		843.2	775.8
		840.3	770.3
out-of-plane CH a-bend	736.7	730.9	

^aReference 5.

and 1075.6 cm^{-1} adjacent to the ν_{10} (CH_2 wag) vibration mode of cyclopropane increased linearly with the concentration of iron. A correlation was found between the absorptions at 1091.9 and 1075.6 cm^{-1} and a broad absorption band in the CH stretching region at 2761.4 cm^{-1} (Figure 3). Both of these absorptions are sensitive to photolysis by visible light at $\lambda \geq 500\text{ nm}$ (Figures 4 and 5), as shown by the disappearance of both bands during photolysis. The CH stretching frequency associated with d has been shifted to a frequency lower than that of uncomplexed cyclopropane by more than 100 cm^{-1} . The doubly degenerate ν_{10} (CH_2 wag) vibration mode of cyclopropane has been shifted by more than 50 cm^{-1} and split into two peaks at 1091.9 and 1075.6 cm^{-1} . These results and the concentration studies suggest that the d bands arise from a strongly interacting complex between iron and two cyclopropane molecules (Scheme 2). When deuterated cyclopropane was used, absorptions from the deuterated species were not observed, presumably due to a lower transition moment. The infrared frequencies measured for this complex are summarized in Table 7. A comparison with the 1:1 iron–

Table 6. FTIR Frequencies (cm⁻¹) for Allene, HFeCH=C=CH₂, FeH₂(H₂C=C=CH₂), and FeH₂^a

vibrational mode	allene ^b	HFeCH=C=CH ₂ ^b	FeH ₂ (H ₂ C=C=CH ₂) (c)	FeH ₂ ^c
C=C=C asym stretch	1955.4	1832.0	1897.8	
Fe-H stretch		1737.7	1658.2	1661

^a The most intense frequencies are given in boldface type. ^b Reference 12. ^c Reference 13.

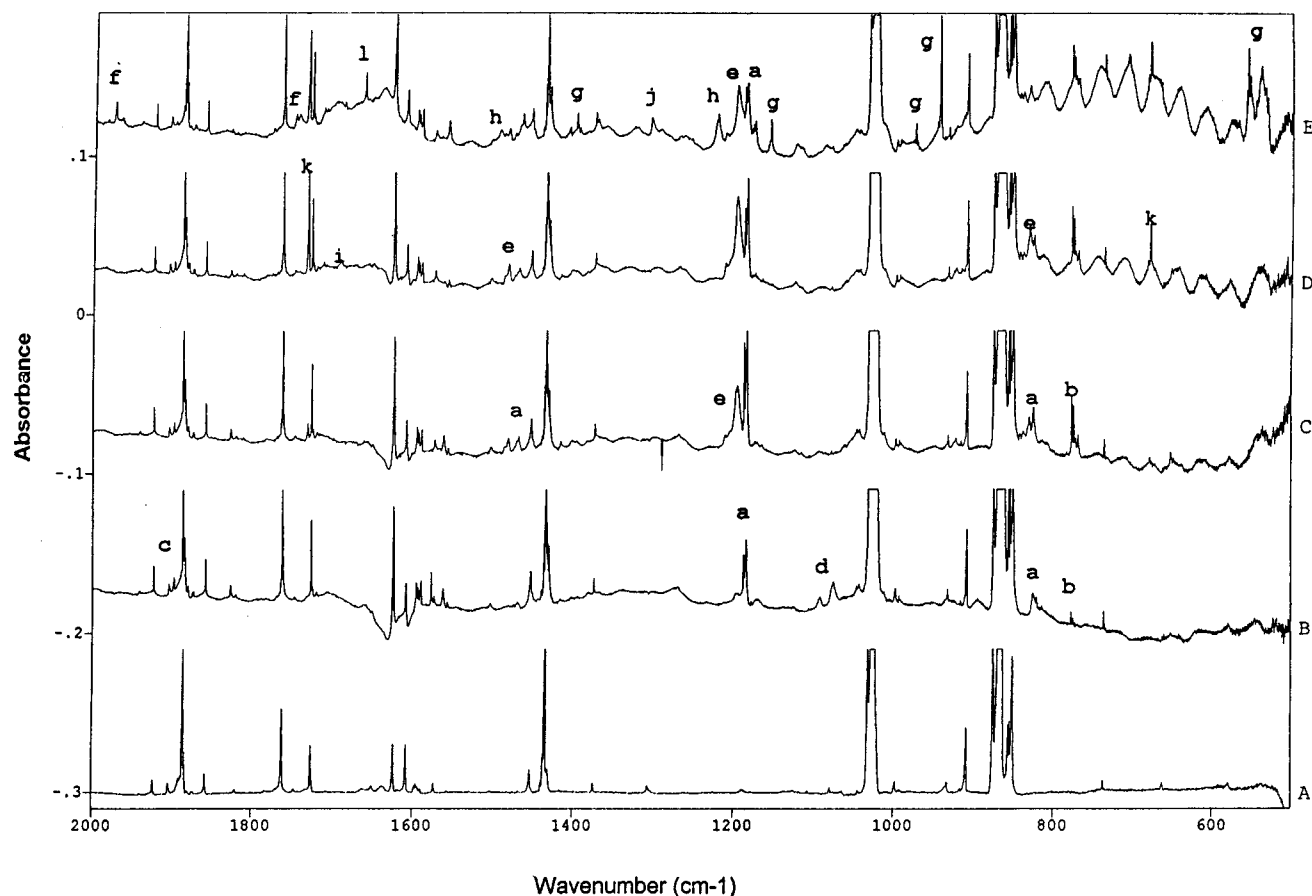


Figure 4. Wavelength-dependent photolysis study of a Fe/C₃H₆Ar matrix: (A) Fe/C₃H₆/Ar = 0/11/1000; (B) Fe/C₃H₆Ar = 12/10/1000; (C) photolysis of B with $\lambda \geq 500$ nm; (D) photolysis of B with $\lambda \geq 400$ nm; (E) photolysis of B with $360 \leq \lambda \leq 280$ nm.

Table 7. FTIR Frequencies (cm⁻¹) for the Fe(C₃H₆)₂ Complex^a

vibrational mode	Fe(C ₃ H ₆) ₂ complex (d)
CH stretch	2788.22
	2768.1
	2763.3
	2761.4
	2755.5
CH ₂ wag	1091.9
	1075.6

^a The most intense frequencies are given in boldface type.

cyclopropane adduct can be seen in Table 2, where the frequency shifts of free cyclopropane are also presented.

An absorption attributed to e (Figure 2) appeared as a broad shoulder adjacent to the 1196.0 cm⁻¹ absorption assigned to a. Since these absorptions occur in the CH₂ scissoring region of transition-metal–olefin π complexes, this indicates that e must be similar in structure to a. The absorption assigned to e also increased linearly with iron concentration. Photolysis using visible light ($\lambda \geq 500$ nm) caused the band attributed to e to increase at a faster rate than a. This absorption continued to increase during irradiation at $\lambda \geq 400$ nm, while peak a began to bleach at this wavelength.

Table 8. FTIR Frequencies (cm⁻¹) for Fe(C₂H₄)₃, Fe(C₂D₄)₃, Fe(C₂H₄)₂, and Fe(C₂D₄)₂ in Solid Argon^a

vibrational mode	obsd Fe(C ₂ H ₄) ₃ (e)	obsd Fe- (C ₂ D ₄) ₃ (e)	Fe(C ₂ H ₄) ₂ ⁴	Fe(C ₂ D ₄) ₂
C=C stretch	1486.6 (sh) 1485.1 (sh) 1481.4		1491.2	1334.7 1329.7
CH ₂ scissors	1195.97	939.2	1221.4	944.0
CH ₂ wag	830.9			

^a The most intense frequencies are given in boldface type.

Using data from previous studies,⁶ peak e has been assigned to the ethylene π complex $\text{Fe}(\text{C}_2\text{H}_4)_3$. Table 8 lists the infrared frequencies assigned to $\text{Fe}(\text{C}_2\text{H}_4)_3$ and $\text{Fe}(\text{C}_2\text{D}_4)_3$ along with the frequencies for $\text{Fe}(\text{C}_2\text{H}_4)_2$ from the earlier study.⁶ The C=C stretching frequency at 1481.4 cm^{-1} and the CH_2 scissoring frequency of 1196.0 cm^{-1} are in agreement with absorptions observed for $\text{Fe}(\text{C}_2\text{H}_4)_2$, $\text{Ni}(\text{C}_2\text{H}_4)_n$,⁷ $\text{Cu}(\text{C}_2\text{H}_4)_n$,⁸ and $\text{Pd}(\text{C}_2\text{H}_4)_n$,⁹ where

- (6) Kafafi, Z. H.; Hauge, R. H.; Margrave, J. L. *J. Am. Chem. Soc.* **1985**, *107*, 7550.
(7) Ozin, G. A.; Power, W. J.; Upton, T. H.; Goddard, W. A., III. *J. Am. Chem. Soc.* **1978**, *100*, 4750.
(8) Ozin, G. A.; Huber, H.; McIntoch, D. *Inorg. Chem.* **1977**, *16*, 3070.
(9) Huber, H.; Ozin, G. A.; Power, W. J. *Inorg. Chem.* **1977**, *16*, 9797.

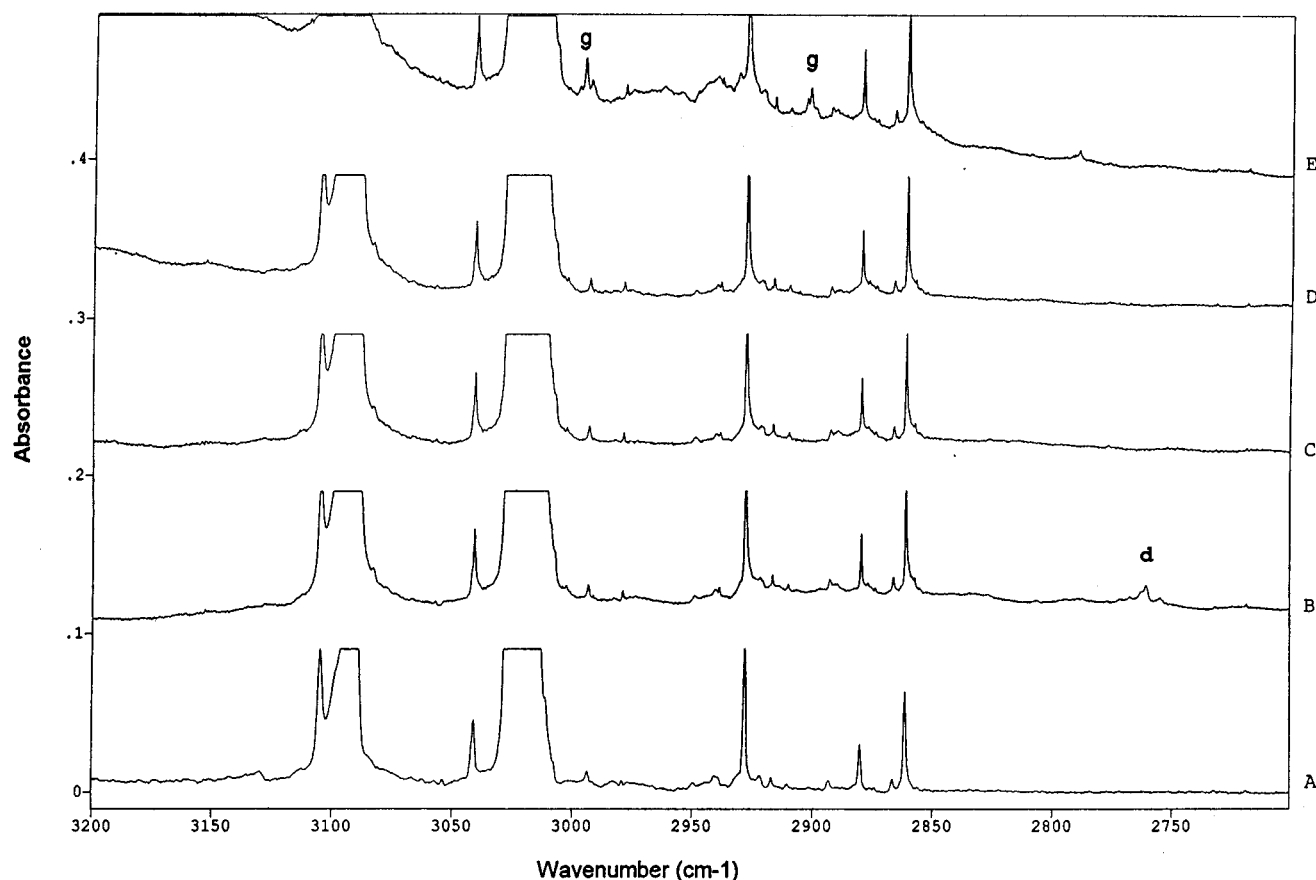


Figure 5. Wavelength-dependent photolysis study of a Fe/C₃H₆/Ar matrix: (A) Fe/C₃H₆/Ar = 0/11/1000; (B) Fe/C₃H₆/Ar = 12/10/1000; (C) photolysis of B with $\lambda \geq 500$ nm; (D) photolysis of B with $\lambda \geq 400$ nm; (E) photolysis of B with $360 \geq \lambda \geq 280$ nm.

$n = 1-3$. Loss of ethylene from Fe(C₂H₄)₃ to yield Fe(C₂H₄)₂ was observed during UV photolysis (280 nm $\leq \lambda \leq 360$ nm).

Photolysis Products. Broad-band irradiation experiments were carried out by photolyzing a Fe/C₃H₆/Ar matrix (molar ratio 12.8:10:1000) in the visible and ultraviolet regions to support the conclusions reached from the concentration studies. Spectral changes observed during the photolyses are presented as difference spectra. The wavelength-dependent photolysis behavior of the products is illustrated in Figures 4 (2000–500 cm⁻¹) and 5 (3200–2700 cm⁻¹). The sequence of the photolysis experiments was $\lambda \geq 500$ nm, $\lambda \geq 400$ nm, and 280 nm $\leq \lambda \leq 360$ nm.

The 1:1 iron–cyclopropane adduct was unchanged during photolysis using visible light but disappeared completely during UV photolysis (280 nm $\leq \lambda \leq 360$ nm). The spectral changes observed during UV photolysis are presented in Figure 6 (1040–1010 cm⁻¹, ν_{10} (CH₂ wag region)). Spectral changes resulting from photolysis of the minor products a–e are presented in Figures 7 (1250–500 cm⁻¹), 8 (2000–1250 cm⁻¹), and 9 (3400–2700 cm⁻¹). Thus, when the matrix was exposed to filtered light ($\lambda \geq 500$ nm) from a mercury lamp, peaks resulting from products a, b, and e, Fe(C₂H₄)₃, grew in intensity while those from c, (FeH₂)(H₂C=C=CH₂), were slightly diminished. Absorptions assigned to d, the Fe(C₃H₆)₂ complex, disappeared completely. Photolysis using shorter wavelength light ($\lambda \geq 400$ nm) caused additional enhancement of e, while absorption bands of a began to diminish.

Table 9. FTIR Frequencies (cm⁻¹) for the Isotopomers of Ethynyliron Hydride and Methane–Ethynyliron Hydride Complex in Solid Argon^a

vibrational mode	HFeC ₂ H ^b	DFeC ₂ D ^b	obsd (HFe–C ₂ H)(CH ₄) (f)	obsd (DFe–C ₂ D)(CD ₄) (f)
C–H stretch	3276.2	2432.8	3275.1	
C=C stretch	1976.4 1974.8	1862.7 1861.0	1975.1 1966.6	1861.5
Fe–H stretch	1765 1762.6	1269.4 1267.2	1747.3 1742.9	1256.9 1254.2
Fe–C stretch				

^a The most intense frequencies are given in boldface type.

^b Reference 6.

UV photolysis of the π complexes a, e, and b led to bleaching of these bands with the concomitant formation of new bands that can be assigned to the ethynyliron–hydride–methane complex (labeled peak f in Figure 4), methylvinyliron (labeled peak g in Figures 4, 5, and 8), and Fe(C₂H₄)₂ (labeled peak h in Figures 4 and 7).

The FTIR frequencies and mode assignments for the ethynyliron–hydride–methane complex are listed in Table 9 along with those of ethynyl iron hydride. The FTIR frequencies observed after UV photolysis of vinylmethyliron are listed in Table 10 along with the deuterated species. Spectral data for vinyliron hydride, vinyliron hydroxide, and vinylmethylnickel are provided for comparison. Frequencies for the π complexes Fe(C₂H₄)₂, Fe(C₂D₄)₂, and the photolysis product h are shown in Table 11.

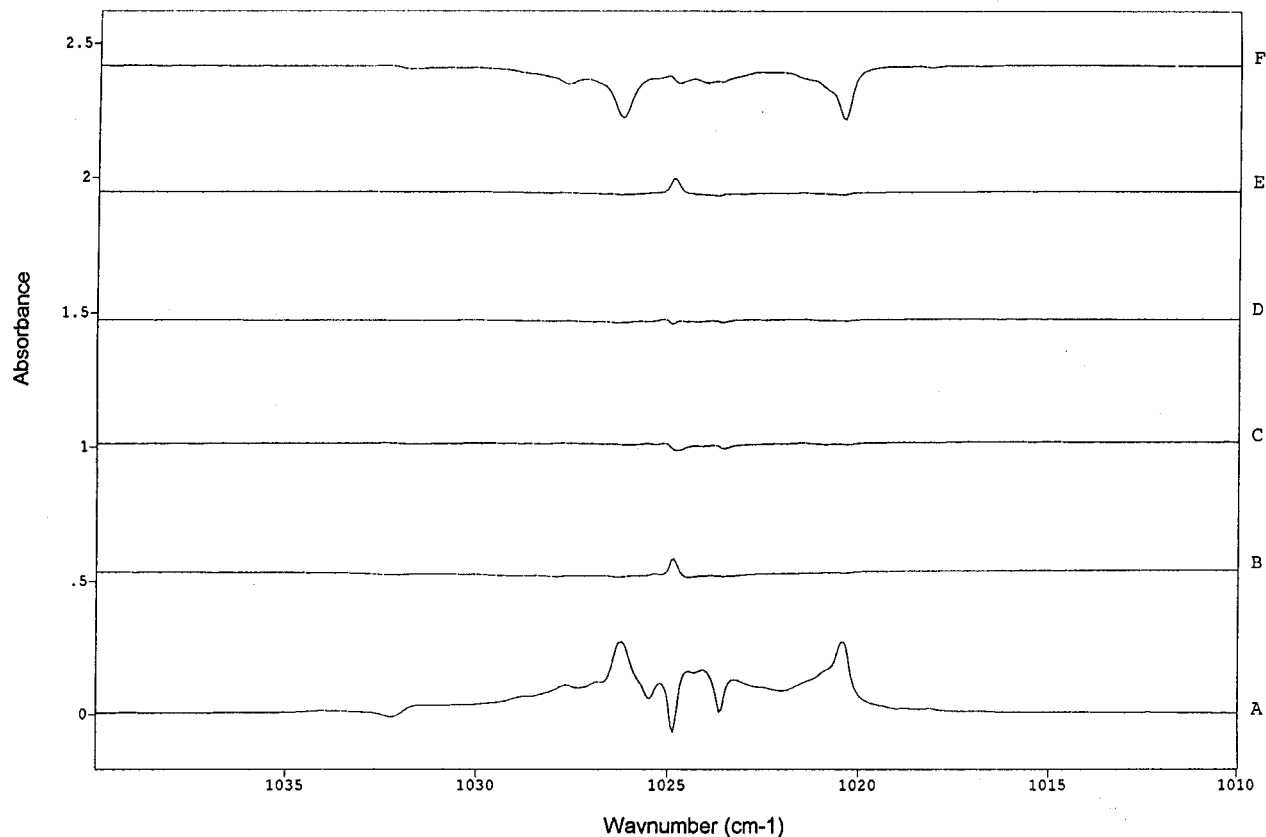


Figure 6. Photolysis study of a Fe/C₃H₆/Ar matrix: (A) Fe/C₃H₆/Ar = 12.8/10/1000; (B) after 20 min photolysis with $\lambda = 500$ nm; (C) after 20 min photolysis with $\lambda \geq 400$ nm; (D) after 40 min photolysis with $\lambda \geq 400$ nm; (E) after 60 min photolysis with $\lambda \geq 400$ nm; (F), after 20 min photolysis with $360 \geq \lambda \geq 280$ nm.

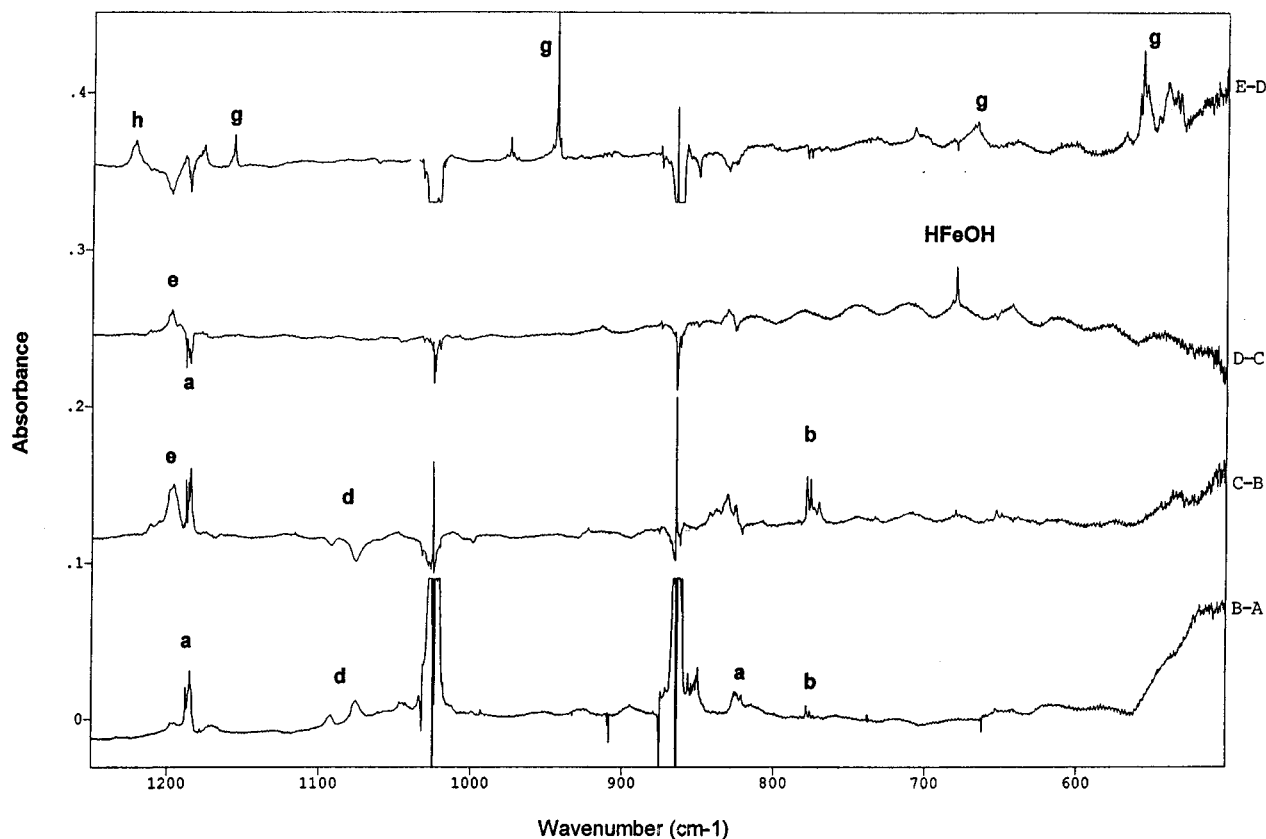


Figure 7. Difference spectra for a photolysis study of a Fe/C₃H₆/Ar matrix (spectra A and B are not shown): (A) Fe/C₃H₆/Ar = 0/10/1000; (B) Fe/C₃H₆/Ar = 12.8/10/1000; (C) photolysis with $\lambda \geq 500$ nm; (D) photolysis with $\lambda \geq 400$ nm; (E) photolysis with $360 \geq \lambda \geq 280$ nm.

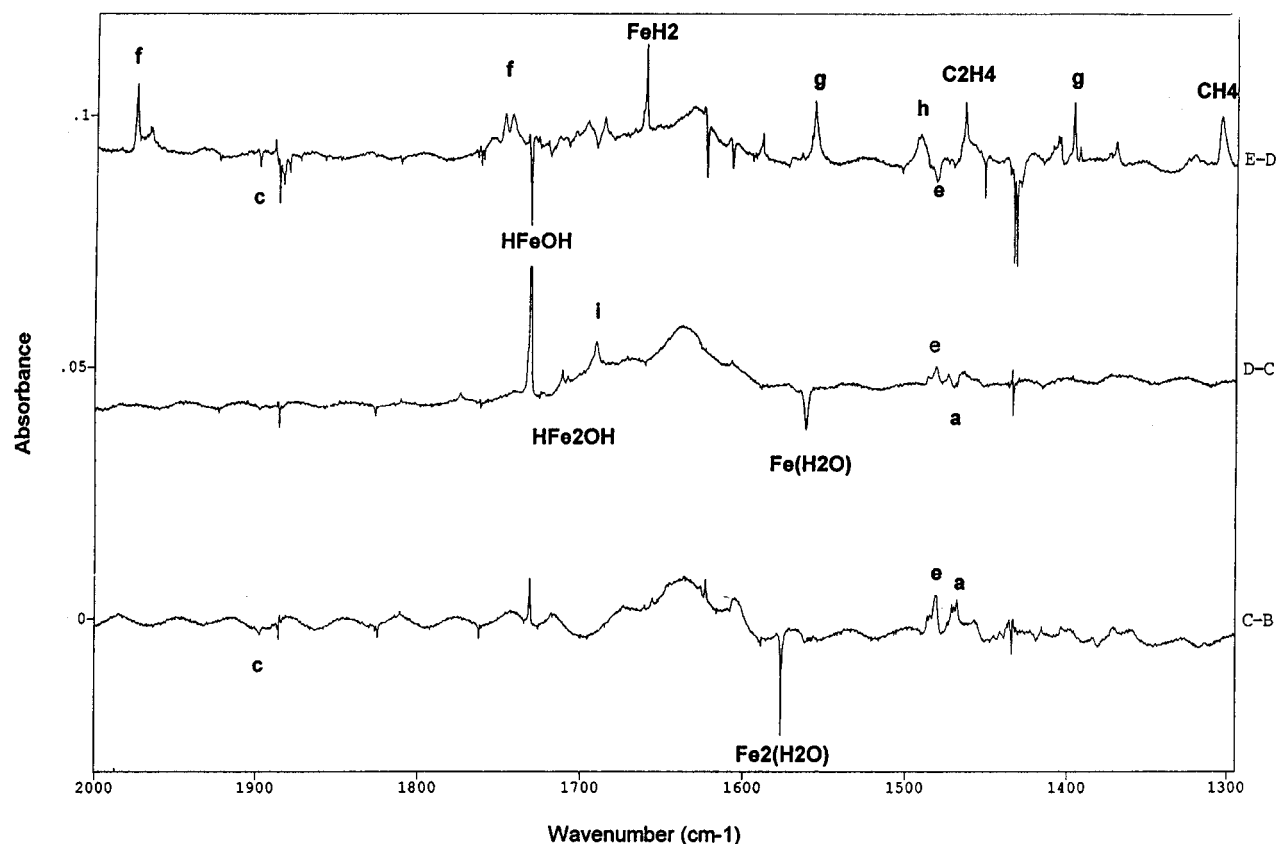


Figure 8. Difference spectra for photolysis of $\text{Fe}/\text{C}_3\text{H}_6/\text{Ar} = 12.8/10/1000$ in the $1300\text{--}2000\text{ cm}^{-1}$ region: (A) $\text{Fe}/\text{C}_3\text{H}_6/\text{Ar} = 0/10/1000$; (B) $\text{Fe}/\text{C}_3\text{H}_6/\text{Ar} = 12.8/10/1000$; (C) after 10 min photolysis with $360 \geq \lambda \geq 280\text{ nm}$; (D) after 10 min photolysis with $\lambda \geq 400\text{ nm}$; (E) after 10 min photolysis with $360 \geq \lambda \geq 280\text{ nm}$.

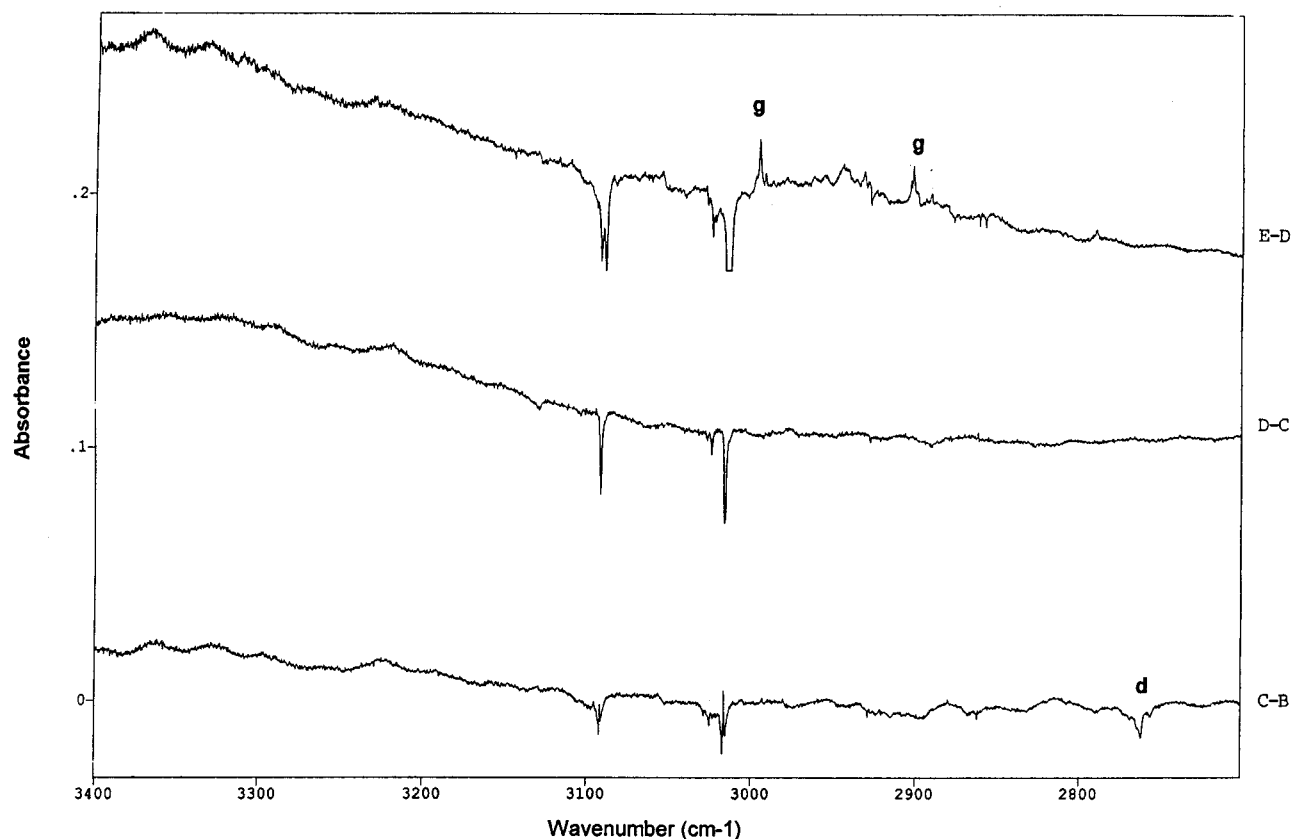


Figure 9. Difference spectra for photolysis of $\text{Fe}/\text{C}_3\text{H}_6/\text{Ar} = 12.8/10/1000$ in the $2700\text{--}3400\text{ cm}^{-1}$ region: (A) $\text{Fe}/\text{C}_3\text{H}_6/\text{Ar} = 0/10/1000$; (B) $\text{Fe}/\text{C}_3\text{H}_6/\text{Ar} = 12.8/10/1000$; (C) after 10 min photolysis with $360 \geq \lambda \geq 280\text{ nm}$; (D) after 10 min photolysis with $\lambda \geq 400\text{ nm}$; (E) after 10 min photolysis with $360 \geq \lambda \geq 280\text{ nm}$.

Table 10. FTIR Frequencies (cm^{-1}) for $\text{H}_3\text{C}_2\text{FeH}$, $\text{H}_3\text{C}_2\text{FeOH}$, $\text{H}_3\text{C}_2\text{FeCH}_3$, and $\text{H}_3\text{C}_2\text{NiCH}_3$ in Solid Argon^a

vibrational mode	$\text{H}_3\text{C}_2\text{FeH}^b$	$\text{H}_3\text{C}_2\text{FeOH}^c$	obsd $\text{H}_3\text{C}_2\text{Fe-CH}_3$ (g)	$\text{H}_3\text{C}_2\text{Ni-CH}_3^d$
CH_2 a-stretch	2999.5		2996.1	
CH stretch	2923.1	2917.1	2921.2	2933.9 2875.3
CH_2 s-stretch	2901.6		2902.4	
FeH stretch	1696.6			
C=C stretch	1556.3	1556.3	1557.1	
CH_2 scissors	1399.1		1397.3	
CH_3 deformation			1155.9	1163.0 1143.6
CH_2 rock	1019.0	1019.0		
HCFe bend	972.9		974.4	
CH_2 wag	944.2	944.2 946.4 948.1	943.8	937.7
CH_3 rock			666.8	661.9
Fe-C stretch	507.2	541.7	558.7 556.4 554.0 539.2 534.3 531.1	

vibrational mode	$\text{D}_3\text{C}_2\text{FeD}^b$	obsd $\text{D}_3\text{C}_2\text{FeCD}_3$ (g)
CD_2 a-stretch	2264.5	2261.4
CD stretch	2175.3	2183.5
CD_2 s-stretch	2150.5	2154.1
FeD stretch	1220.5	
C=C stretch	1477.4	1475.8
CD_2 scissors	1063.1	1048.0
CD_3 deformation		904.7
CD_2 rock	713.5	
CD_2 wag	737.4	738.6
Fe-C stretch	491.0	514.2

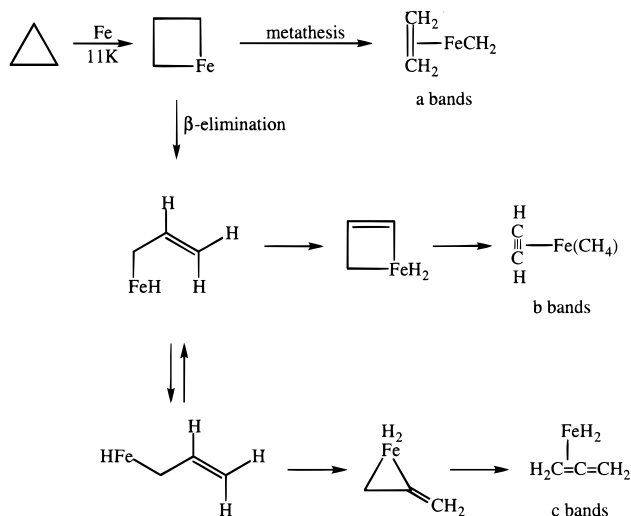
^a The most intense frequencies are given in boldface type.^b Reference 6. ^c Reference 14. ^d Reference 2.**Table 11.** FTIR Frequencies (cm^{-1}) for the Isotopomers of $\text{Fe}(\text{CH}_2\text{CH}_2)_2$ in Solid Argon^a

vibrational mode	$\text{Fe}(\text{C}_2\text{H}_4)_2^b$	$\text{Fe}(\text{C}_2\text{D}_4)_2^b$	obsd $\text{Fe}-(\text{C}_2\text{H}_4)_2$ (h)	obsd $\text{Fe}-(\text{C}_2\text{D}_4)_2$ (h)
CH_2 a-stretch	3052.3		3052.5	
CH_2 s-stretch	2974.2		2976.0	
C=C stretch	1491.2	1334.7 1329.7	1493.6 1492.1	1334.7
CH_2 scissors	1221.4	944.0	1221.7	943.7

^a The most intense frequencies are given in boldface type.^b Reference 6.

Discussion

In contrast to the reaction of nickel with cyclopropane, where an unligated four-membered metallacycle² was formed, the major cocondensation product from iron was a weakly complexed iron-cyclopropane adduct. This observation is consistent with earlier studies where iron was found to interact with acetylene¹⁰ and ethylene through the hydrogen-bonded complexes $\text{Fe}\cdots\text{HCCH}$

Scheme 1

and $\text{Fe}\cdots\text{HC}=\text{CH}_2$, respectively. Evidence for a π -complexed adduct of iron with acetylene or ethylene was not found. The classical π complexes known for many transition-metal-ethylene systems could only be isolated from iron and ethylene when more than one ethylene was bound to the metal as in $\text{Fe}(\text{C}_2\text{H}_4)_2$. Nickel, however, interacts readily with acetylene and ethylene to form π complexes. Theoretical calculations will probably be required to delineate the hydrogen-bonded complexes that lead to the small perturbations in the ν_2 (CH_2 rock), ν_{10} (CH_2 wag), ν_9 (CH_2 scissor), ν_6 (CH_2 a-stretch), and ν_8 (CH_2 s-stretch) frequencies of cyclopropane.

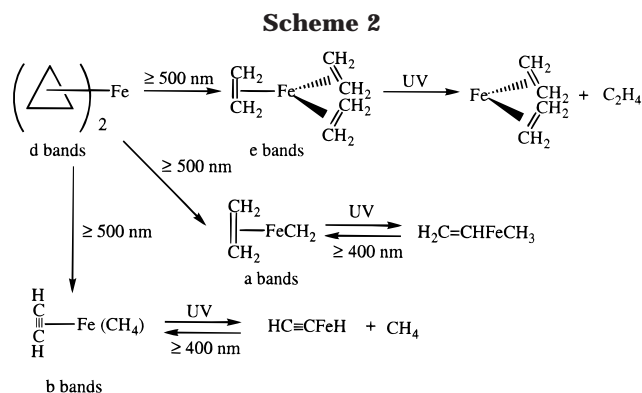
The formation of products from spontaneous reactions (peaks a–e), although much less abundant than the hydrogen-complexed adducts, contrasts with earlier studies with strain-free hydrocarbons where photolysis was required for bond activation. A possible explanation is that the spontaneous reactions arise from iron atoms that either are kinetically energetic or are in an excited state. Calculations indicate that approximately 0.4% of the iron atoms exiting the furnace are in an excited s^5F electronic state. The lifetime of this state is calculated to be 500–1000 s.¹ Thus, no loss of excitation is expected in the time required for the metal to reach the matrix surface. Pathways which account for the formation of products a–c are illustrated in Scheme 1. This scheme requires the metastable ferracyclobutane to be the initially formed species. Spontaneous rearrangement of the ferracyclobutane via a metathesis reaction would yield the carbene complex (a bands). Formation of the remaining products (b and c) can be explained by a series of steps initiated by a β -hydride elimination.

The thermal populations of first-row transition-metal $3d^{n+1}4s^1$ states relative to the $3d^n4s^2$ states are given in Table 12. The temperatures listed in the table correspond to a metal vapor pressure of 10^{-6} atm. Radiative transitions from the $3d^{n+1}4s^1$ state to the $3d^n4s^2$ state are electric dipole forbidden; thus, all $3d^{n+1}4s^1$ states are long-lived ones. As a consequence, excited-state reactions on an inert matrix surface with other molecules are possible for Sc, Ti, V, Cr, Fe, Co, and Ni. For Cr, Ni, and Cu, the reaction of the $3d^{n+1}4s^1$ state will probably dominate. The spontaneous reaction observed earlier when atomic nickel was reacted with

(10) Kline, E. S.; Kafafi, Z. H.; Hauge, R. H.; Margrave, J. L. *J. Am. Chem. Soc.* **1985**, *107*, 7559.(11) Shimanouchi, T. *Tables of Molecular Vibrational Frequencies*; 1971; Vol. 1, pp 120–121, 145–146.(12) Ball, D. W.; Pong, R. G. S.; Kafafi, Z. H. *J. Am. Chem. Soc.* **1993**, *115*, 2864.(13) Rubinovitz, R.L.; Nixon, E.R. *J. Phys. Chem.* **1986**, *90*, 1940–1944.(14) Kafafi, Z. H.; Hauge, R. H.; Billups, W. E.; Margrave, J. L. *J. Am. Chem. Soc.* **1987**, *109*, 4775.

Table 12. Thermal Population of the $4d^{n+1}3s^1$ Electronic State of First-Row Transition Metals^a

transition metal	temp (K)	% population
Ca	785	0
Sc	1453	0.2
Ti	1833	1
V	1945	19.75
Cr	1530	99.82
Mn	1132	0
Fe	1594	0.25
Co	1639	4.77
Ni	1646	42.62
Cu	1394	100
Zn	564	0

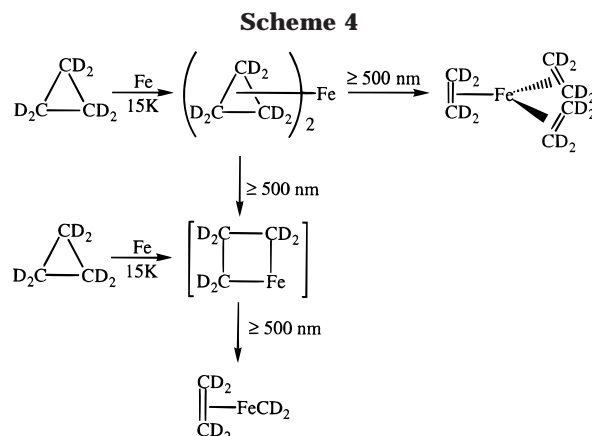
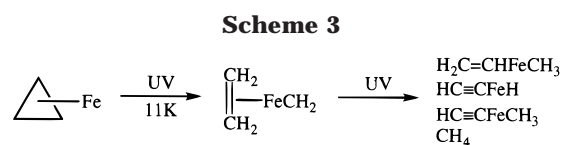
^a NIST Atomic Spectroscopic Database, version 1.0, 1996.

cyclopropane to give the metallacycle might have resulted from a reaction of the $3d^94s^1$ state. The greater electronic excitation energy (~ 20 kcal) that the $3d^74s^1$ state of iron brings to a reaction suggests that a greater reactivity would be associated with this metal.

Reactions of Atomic Iron with Dicyclopentadiene. The iron–dicyclopentadiene complex (product d) may involve bonding through the electron-rich σ bonds of the hydrocarbon. The interaction of two cyclopentadiene molecules with iron is clearly much stronger than for a single cyclopentadiene, as indicated by the larger shifts of the hydrogen stretching modes. This interaction may be sufficient to elevate the iron atom to the $3d^74s^1$ state, since the yield of $\text{Fe}(\text{C}_2\text{H}_4)_3$ (product e) could be enhanced by photolysis using visible light ($\lambda \geq 500$ nm) of the adduct, as illustrated in Scheme 2.

Photolytic Reactions of Atomic Iron with Cyclopropane. Photolysis studies carried out on the $\text{Fe}/\text{C}_3\text{H}_6$ system in solid argon showed that the weakly bonded iron–cyclopropane complex was unaffected by irradiation using either a $\lambda \geq 500$ or a $\lambda \geq 400$ nm cutoff filter. However, UV photolysis ($280 \text{ nm} \leq \lambda \leq 360 \text{ nm}$) led to bleaching of the peaks associated with the adduct along with the concomitant formation of new peaks in various regions of the FTIR spectrum that are associated with photoproducts. The photoproducts are thought to arise from a series of reactions in which the coordinatively unsaturated iron inserts into the C–H bonds of the coordinated ligands ethylene and acetylene (Scheme 3).

Reactions of Atomic Iron with Deuterated Cyclopropane. A strong isotope effect is in evidence when



iron atoms are cocondensed with deuterated cyclopropane in an argon matrix at 15 K. Results of this study are outlined in Scheme 4. The formation of $(\text{C}_2\text{D}_4)\text{FeCD}_2$ (the only product) may be explained by metathesis of a transient ferracyclobutane which would be formed by insertion of the $[a^5\text{F}(3d^74s^1)]$ state of iron into a carbon–carbon bond of the hydrocarbon as discussed earlier. The striking feature of this study is the absence of products resulting from C–H bond activation (β -elimination) or the formation of a 1:1 $\text{C}_3\text{D}_6\text{--Fe}$ adduct. Photolysis using visible light ($\lambda \geq 500$ nm) led to an enhancement of the peaks assigned to $(\text{C}_2\text{D}_4)\text{FeCD}_2$. Formation of the ethylene π complex $\text{Fe}(\text{C}_2\text{D}_4)_3$ was also observed during photolysis using visible light ($\lambda \geq 500$ nm and $\lambda \geq 400$ nm). Evidence for iron dicyclopentadiene, $\text{Fe}(\text{C}_3\text{D}_6)_2$, was not observed in the FTIR spectra during cocondensation of the reactants, although its existence is inferred from the photochemistry at $\lambda \geq 500$ nm. The failure to observe this species is attributed to the weakness of the absorptions exhibited by the deuterated iron–dicyclopentadiene complex.

Summary of Results

1. Ground-state atomic iron forms a weakly bound complex with cyclopropane. UV irradiation of this complex yields $\text{C}_2\text{H}_3\text{FeCH}_3$, HFeC_2H , and methane.

2. A strongly interacting iron–dicyclopentadiene complex was observed. This species exhibits infrared frequencies that are characteristic of an agostic type hydrogen interaction.

3. The spontaneous formation of $\text{C}_2\text{H}_4\text{FeCH}_2$, $[\text{Fe}(\text{C}_2\text{H}_2)][\text{CH}_4]$, and $(\text{FeH}_2)(\text{H}_2\text{C}=\text{C}=\text{CH}_2)$ can be explained in terms of a thermally generated excited state $[a^5\text{F}(3d^74s^1)]$ of iron reacting with cyclopropane.

Acknowledgment. We gratefully acknowledge financial support from the National Science Foundation and the Robert A. Welch Foundation.

OM990483J